Journal of Power Sources 214 (2012) 113–118

Contents lists available at SciVerse ScienceDirect

Journal of Power Sources

journal homepage: www.elsevier.com/locate/jpowsour

Effect of structural compatibility of dye and hole transport material on performance of solid-state dye-sensitized solar cells

Wei-Chih Chen [a], Chia-Yuan Chen [b], Chun-Guey Wu [b,**], Kuo-Chuan Ho [a,c], Leeyih Wang [a,d,*]

[a] Institute of Polymer Science and Engineering, National Taiwan University, Taipei 10617, Taiwan
[b] Department of Chemistry, National Central University, Jung-Li 32054, Taiwan
[c] Department of Chemical Engineering, National Taiwan University, Taipei 10617, Taiwan
[d] Center for Condensed Matter Sciences, National Taiwan University, Taipei 10617, Taiwan

HIGHLIGHTS

- High structural compatibility of dye and HTM enhances the regeneration of dye.
- P3HT can act as a hole conductor and co-sensitizer in an ss-DSC.
- Ultrathin CYC-B11/P3HT ss-DSC exhibits a power conversion efficiency of 3.66%.

GRAPHICAL ABSTRACT

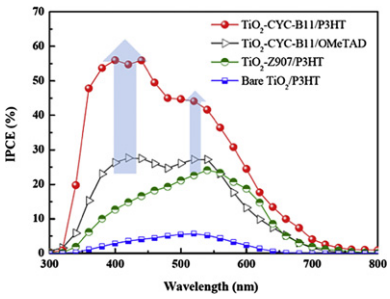

ARTICLE INFO

Article history:
Received 17 January 2012
Received in revised form
26 April 2012
Accepted 29 April 2012
Available online 5 May 2012

Keywords:
Solid-state dye-sensitized solar cells
Structural compatibility
P3HT
Impedance

ABSTRACT

Solid-state dye-sensitized solar cells (ss-DSCs) are fabricated using Z907 or its thiophene derivative, CYC-B11, as a dye, and poly(3-hexylthiophene) (P3HT) or (2,2′,7,7′-tetrakis-(*N*,*N*-di-*p*-methoxyphenylamine) 9,9′)-spirobifluorene (OMeTAD) as a hole transport material (HTM). The effect of the structural compatibility of dye molecules with HTM on device performance is investigated. The CYC-B11/P3HT device has a much higher short-circuit current density than Z907/P3HT and CYC-B11/OMeTAD devices. Results from the incident photo-to-electron conversion efficiency and impedance measurements support the use of P3HT, in place of OMeTAD, as HTM markedly increases the photocurrent throughout the absorption spectrum of CYC-B11 and significantly reduces the charge-transfer resistance at the TiO_2/dye/HTM interface. As a result, the CYC-B11/P3HT ss-DSC that is fabricated from a thin (0.5 μm) mesoporous TiO_2 layer exhibits an outstanding power conversion efficiency of 3.66%.

1. Introduction

Solid-state dye-sensitized solar cells (ss-DSCs) have attracted considerable attention in recent years because of the simplicity of their fabrication process, good device stability and need for less sealing material than required by liquid-state DSCs [1–3]. Although the power conversion efficiency (PCE) of ss-DSCs has recently been substantially improved to be greater than 5% [4,5], this value is still much lower than that of their liquid-state DSC counterparts, mainly because of the short diffusion length of the charge carriers [6] and the poor regeneration efficiency of the dyes [7]. The inefficient dye regeneration can increase the probability of undesirable recombination between the electrons on TiO_2 and dye cations, reducing both open-circuit voltage (V_{OC}) and short-circuit current density (J_{SC}) [7,8]. Accordingly, enhancing the hole-transfer efficiency at the

* Corresponding author. Center for Condensed Matter Sciences, National Taiwan University, Taipei 10617, Taiwan. Tel.: +886 2 3366 5279; fax: +886 2 2369 6221.
** Corresponding author.
E-mail addresses: t610002@cc.ncu.edu.tw (C.-G. Wu), leewang@ntu.edu.tw (L. Wang).

0378-7753/$ – see front matter © 2012 Elsevier B.V. All rights reserved.
doi:10.1016/j.jpowsour.2012.04.093

interface between the dye and hole transport material (HTM) is apparently critical for developing highly efficient ss-DSCs. Durrant et al. [9] studied the TiO_2/dye/triphenylamine-based HTMs heterojunction and demonstrated that the yield of the hole-transfer reaction is determined by the thermodynamic driving force rather than the kinetic competition with the recombination reaction between the oxidized dyes and the injected electrons, because the transfer process proceeds much faster than the recombination process. However, unlike the liquid electrolyte, which can very effectively penetrate into the tiny pores of the TiO_2 layer, solid HTMs have a relatively large molecular size, high viscosity and low fluidity, which usually prevent their complete filling of TiO_2 mesopores. Numerous research groups [7,10–13] have identified the full coverage of a dye-coated TiO_2 surface with HTM and a high pore-filling fraction by HTM as key factors in improving the performance of ss-DSCs. The former facilitates a smooth hole-transfer from oxidized dyes to HTMs [10,11]; the latter shortens the pathway along which the charges move toward the electrodes and increases the average spatial separation of opposite charge carriers [7,12,13], reducing the recombination rate. Besides, the structural compatibility of HTMs and dyes may also influence the physical separation of two materials, thereby changing the reduction efficiency of dye cations.

2. Experimental section

2.1. Materials

Titanium isopropoxide (TTIP, 98%), titanium tetraethoxide (TEOT, 99%) and bis(trifluoromethane) sulfonimide lithium salt (Li-TFSI, 99.95%) were obtained from Acros. Pluronic poly(ethylene oxide)-poly(propylene oxide)-poly(ethylene oxide) triblock copolymer (P123) and 4-*tert*-butylpyridine (*t*BP, 96%) were purchased from Aldrich. Commercial dye, Z907, and 2,2′,7,7′-tetrakis-(*N*,*N*-di-*p*-methoxyphenylamine)9,9′-spirobifluorene (OMeTAD) were supplied by Everlight Chemical Industrial Corp. Ltd. and Luminescence Technology Corp, respectively, and used as received. The ruthenium-dye, CYC-B11, was synthesized and purified according to the procedure published elsewhere [14]. Regioregular poly(3-hexylthiophene) (P3HT) was prepared using the Grignard metathesis approach, providing regiocontrol in each coupling step in the polymeric reaction [15]. The regioregularity was determined by ^1H NMR to be greater than 96%. The number-average molecular weight was 17,000 g mol^{-1} and the polydispersity index was 1.1, based on GPC analysis (THF eluent, polystyrene standard).

2.2. Fabrication of solid-state dye-sensitized solar cells

The fluorine-doped SnO_2 (FTO) (Pilkington, 15 Ω $square^{-1}$) substrates were sequentially cleaned with detergent, deionized water, acetone and isopropyl alcohol in an ultrasonic bath, and then dried in N_2 flow. A precursor solution of titanium isopropoxide/acetylacetone complexes was prepared by mixing titanium isopropoxide (0.284 g) with acetylacetone (0.203 g) in ethanol (5.0 ml). The solution was deposited on a cleaned FTO glass, which was preheated to 450 °C, by the spray pyrolysis method using N_2 as carrying gas at a flow rate of 400 cc min^{-1}. Following deposition, films were calcined at 450 °C for 30 min under air, yielding dense TiO_2 films with a thickness of around 60 nm. Mesoporous TiO_2 (mp-TiO_2) films were then prepared by adding a solution containing concentrated HCl (3.205 g) and titanium ethoxide (4.302 g) to a solution of Pluronic P123 triblock copolymer (1.007 g) in ethanol (15.0 ml). After 3–4 h of vigorously stirring at room temperature, the resulting solution was dip-coated on top of FTO/dense TiO_2 substrates at a speed of 6 cm min^{-1}, followed by rapid thermal treatment at 450 °C for 5 min and then gradual cooling to ambient temperature. The above dip-coating process was repeated five times to yield a porous TiO_2 layer with a thickness of ca. 500 nm. Next, the mesoporous film was calcined at 500 °C for 4 h. After the as-prepared substrates had cooled to 80 °C, they were immersed into a ruthenium-dye (CYC-B11 and Z907) solution (0.3 mM, acetonitrile:*tert*-butanol = 1:1) overnight, followed by rinsing with acetonitrile three times and drying in N_2 flow. The dyed-TiO_2 films were spin-coated with a mixed solution of Li-TFSI (0.1 M) and *t*BP (0.01 M) in *p*-xylene (3500 rpm for 30 s), and dried in N_2 flow. Then, a P3HT (15.0 mg ml^{-1}) or OMeTAD (30.0 mg ml^{-1}) solution in a solvent mixture of *o*-dichlorobenzene and chlorobenzene with a volume ratio of 3:1, was spin-coated (800 rpm for 30 s) to afford HTM, and then heated at 125 °C for 7 min to facilitate the infiltration of HTM into titania pores. Finally, the film was deposited with a thin layer of Au (5 nm)/Ag (100 nm) by thermal evaporation under a vacuum of 10^{-6} torr in an Edwards Auto 306 vacuum evaporation system through a shadow mask to yield ss-DSCs with an active area of 7 mm^2.

2.3. Characterization

UV–vis absorption spectra were taken by a Jasco V-670 UV–Vis spectrophotometer. Cyclic voltammetry (CV) measurements were performed using a CHI 660 Electrochemical Analyzer with a glassy carbon, a Pt plate, and a saturated aqueous Ag/Ag^+ electrode as the working, counter and reference electrodes, respectively, in an anhydrous DMF solution containing 0.1 M *tetra*-*n*-butylammonium hexafluorophosphate at a scan rate of 30 mV s^{-1} under N_2 atmosphere. The reference electrode was calibrated by running the CV of ferrocene without adding analyte to the solution. The morphology and thickness of mesoporous TiO_2 films were examined using a field-emission scanning electron microscope (JSM-6700F, JEOL Company). The current density–voltage (*J*–*V*) characteristics of photovoltaic devices were evaluated with a Keithley 2400 source meter under AM 1.5G solar irradiation obtained from a 300 W Oriel solar simulator, at an intensity of 100 mW cm^{-2}, which was

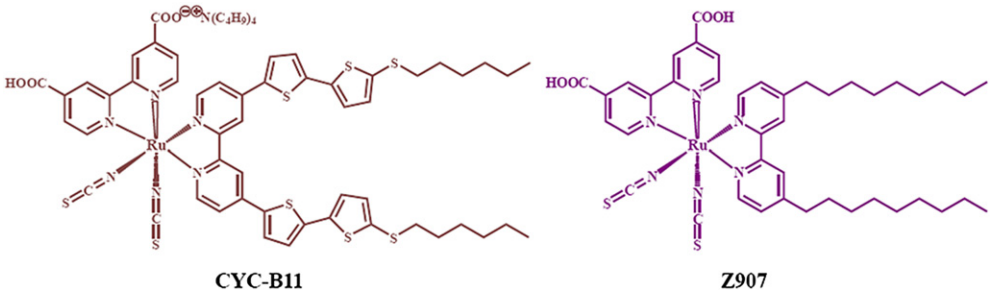

Fig. 1. Molecular structure of CYC-B11 and Z907 dyes.

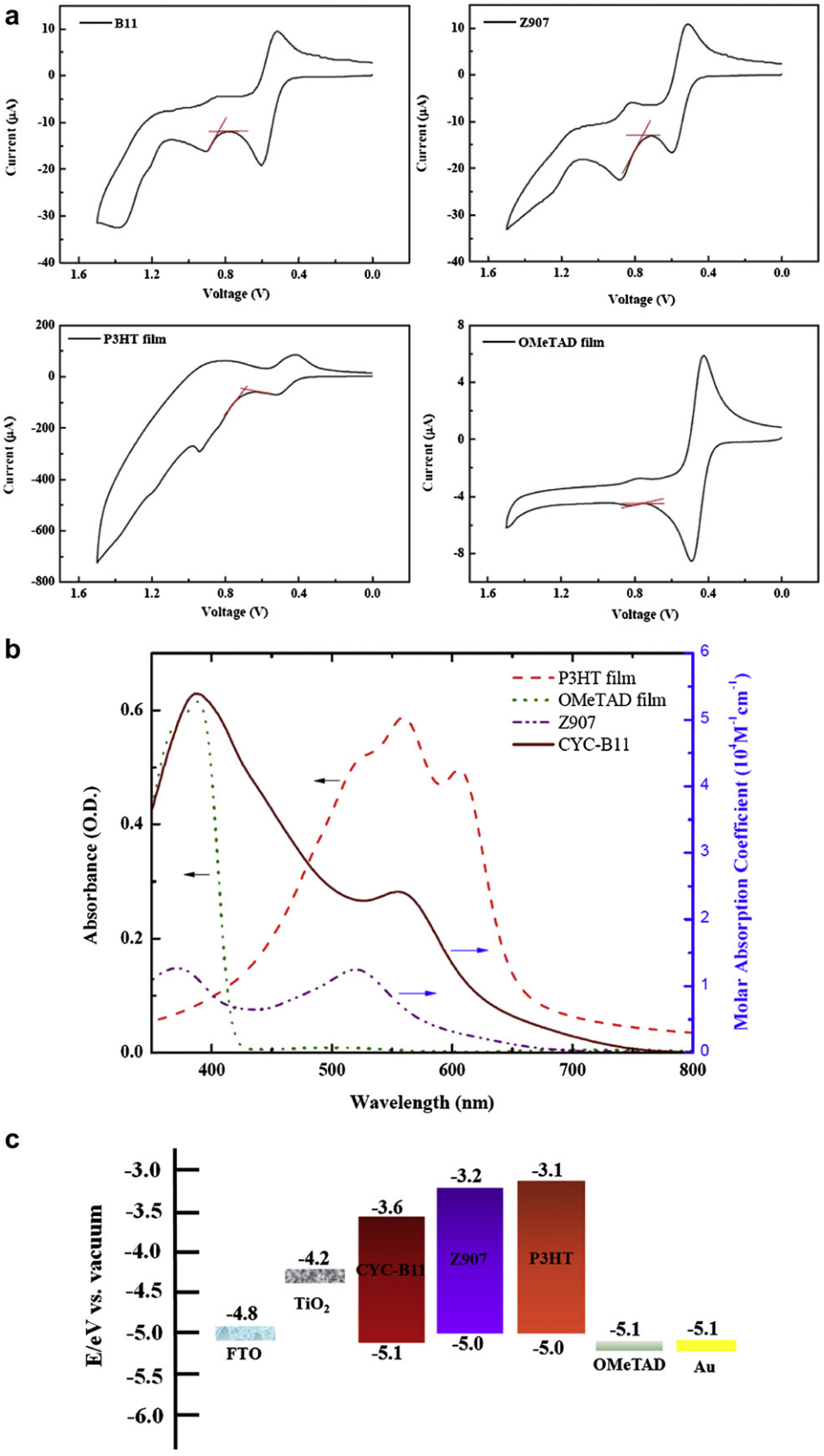

Fig. 2. (a) UV–vis absorption spectra and (b) cyclic voltammograms of CYC-B11, Z907, P3HT and OMeTAD. (c) Schematic energy levels of the components in ss-DSCs.

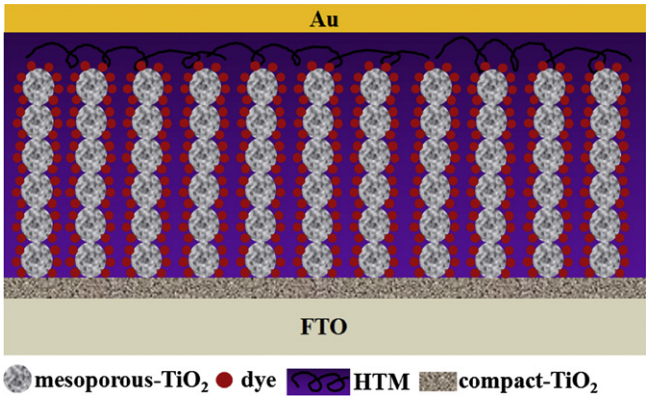

Fig. 3. Schematic structure of ss-DSC device.

calibrated by a mono-Si reference cell with a KG5 filter. The incident photon-to-current conversion efficiency (IPCE) spectra were recorded under illumination by a xenon lamp and a monochromator (TRIAX 180, JOBIN YVON), and the light intensity was calibrated by using an OPHIR 2A-SH thermopile detector. Electrochemical impedance spectroscopy (EIS) was obtained by a PGSTAT 30 potentiostate/galvanostate (Autolab, Eco-Chemie, the Netherlands) equipped with an FRA2 module, under a constant light illumination of 100 mW cm^{-1} and with an applied voltage of 0.01 V.

3. Results and discussion

In this study, Z907 or its thiophene derivative analog (CYC-B11) were adopted as light-harvesting molecules in combination with P3HT or OMeTAD, functioning as HTM, to examine how the compatibility of two materials affects the photovoltaic properties of ss-DSCs. Fig. 1(a) displays the molecular structure of two dye molecules. Energy levels of the highest occupied molecular orbital (HOMO) and the lowest unoccupied molecular orbital (LUMO) of CYC-B11, Z907, P3HT and OMeTAD were determined using both cyclic voltammetry and UV–vis spectrometry [14,16,17]. The cyclic voltammograms of the four compounds are shown in Fig. 2(a), in which ferrocene was used as the internal standard. The HOMO was then calculated from the onset potential of oxidation wave ($E_{ox,onset}$), according to the formula of HOMO $= -[(E_{ox,onset} - E_{Fc+}) + 4.8\ eV]$, where E_{Fc+} denotes the measured oxidation potential of ferrocene and 4.8 eV is the absolute oxidation potential value of ferrocene under vacuum. Moreover, the LUMO can be estimated from the sum of HOMO and optical bandgap, which was determined from the wavelength of absorption onset in the UV–vis spectra in Fig. 2(b). Based on these results, the electronic energy level diagram of each component in ss-DSCs is plotted in Fig. 2(c). The LUMO level of CYC-B11 (−3.6 eV) and Z907 (−3.2 eV) is well above the conduction band edge of TiO_2 (−4.2 eV) [18]. Therefore, electron injection from the LUMO of both dyes into the conduction band of TiO_2 is energetically feasible. In addition, the LUMO of P3HT (−3.1 eV) is higher than that of both dyes, so P3HT can act not only as a hole conductor but also as a co-sensitizer, enhancing the harvesting of sunlight and increasing the photocurrent.

Fig. 3 presents the schematic diagram of the solid-state photovoltaic devices fabricated in this study. A thin layer of compact TiO_2 (~60 nm) was deposited on top of an FTO conducting glass by spray pyrolysis to prevent short-circuiting due to the direct contact of P3HT with anode. The mesoporous TiO_2 layer was then made by dip-coating the FTO/TiO_2 substrate from an ethanol solution that comprised a $(TiOEt)_4$ precursor and an amphiphilic triblock copolymer, P123, which acts as a structure directing agent. Mesopores were formed by the solvent evaporation-induced self-assembly of the titania precursor, followed by calcinating the hybrid film at 500 °C for 60 min to burn out the organic substances [19]. As shown in the SEM image in Fig. 4, the as-prepared porous film has pore sizes of 8–10 nm and a thickness of around 500 nm. A large pore is beneficial to efficiently infiltrating a solid hole conductor, especially for a large-size polymer, into the bottom layer of the porous TiO_2 film. To facilitate the penetration of P3HT into mesoporous TiO_2 film, a low-molecular-weight P3HT (M_n = 17,000 g mol^{-1}) was employed, and high-boiling-point solvents, *o*-dichlorobenzene and chlorobenzene, were utilized to reduce the rate of drying of P3HT solution during the coating process. Moreover, a thin Au/Ag film was adopted as the hole-collecting cathode to increase the optical path length inside the device because Ag has a high reflectivity for visible light.

Fig. 5 plots the *J–V* curves of these ss-DSCs, which were measured in the dark and under AM 1.5G irradiation (100 mW cm^{-2}). Table 1 presents the related photovoltaic data. The CYC-B11/P3HT device exhibits a J_{SC} of 6.71 mA cm^{-2}, which is about 3.6 mA cm^{-2} or 117% higher than that of the Z907/P3HT device, yielding an excellent PCE of 3.66%. Statistical data from ten devices reveal that the CYC-B11/P3HT device has a V_{OC}, J_{SC}, *FF* and PCE of 0.75 ± 0.01 V, 6.93 ± 0.17 mA cm^{-2}, 67.62 ± 2.13% and 3.52 ± 0.07%, respectively. According to the literatures [14,17], the CYC-B11 device has a higher J_{SC} than the Z907 device because CYC-B11 has a broader absorption spectrum and a higher molar absorption coefficient than Z907. However, the increment of J_{SC} in those liquid-electrolyte DSCs is less than 25%, which is much smaller than that in our devices, suggesting other factors may also influence the raise of J_{SC}. To investigate these findings further, a CYC-B11 device using OMeTAD, whose molecular structure lacks thiophene units, as HTM was also fabricated. As shown in Fig. 5 and Table 1, this device has a PCE of 2.13%, which is lower than that reported in the literature

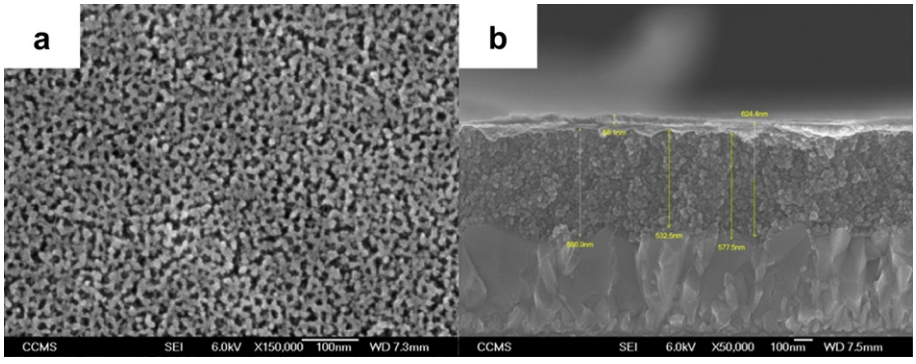

Fig. 4. SEM images of the (a) top view and (b) cross-sectional view of the mesoporous TiO_2 layer deposited on top of a dense-TiO_2/FTO substrate.

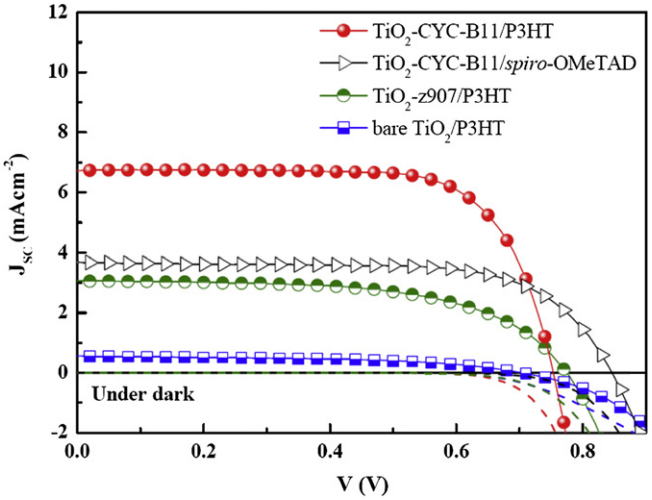

Fig. 5. *J–V* curves of the four solid-state dye-sensitized solar cells based on TiO_2/CYC-B11/P3HT, TiO_2/CYC-B11/OMeTAD, TiO_2/Z907/P3HT and bare TiO_2/P3HT.

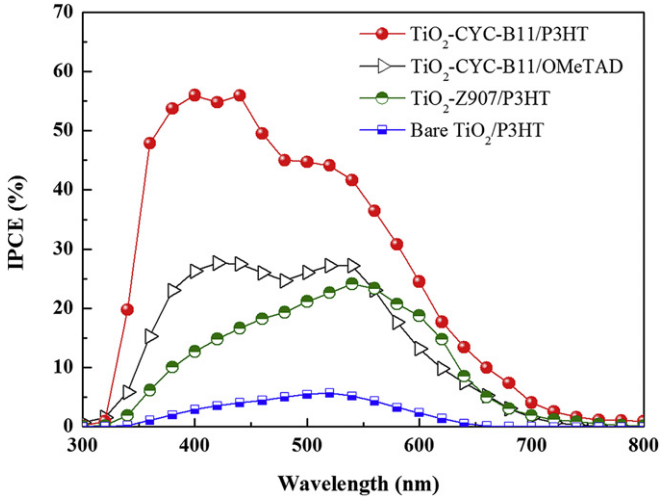

Fig. 6. Incident photon-to-current conversion efficiency (IPCE) spectra of the four solid-state dye-sensitized solar cells based on TiO_2/CYC-B11/P3HT, TiO_2/CYC-B11/OMeTAD, TiO_2/Z907/P3HT and bare TiO_2/P3HT.

[14], because it has a thinner porous TiO_2 film ($\sim$0.5 μm) to ensure high infiltration of HTMs. Obviously, the J_{SC} of P3HT-based device is about 3 mA cm^{-2} higher than that of the OMeTAD-based device. Although both CYC-B11 and P3HT can contribute to the photocurrent in a CYC-B11/P3HT cell, the contribution of P3HT to the J_{SC} in the model device, in which no dye molecules are adsorbed on the TiO_2 surface, is less than 1 mA cm^{-2}, as shown in Fig. 2. This observation implies that the structural compatibility of dye molecule and HTM may importantly determine the J_{SC} of ss-DSCs.

Consistent with the J_{SC} values in Table 1, Fig. 6 shows that CYC-B11/OMeTAD and Z907/P3HT devices have similar IPCE spectra, except in the region 350–470 nm because CYC-B11 has a stronger absorbance than Z907. Replacing OMeTAD with P3HT as the HTM significantly increases the IPCE across the entire absorption spectrum of CYC-B11 instead of the absorption region of P3HT, with a maximum of 55% at 450 nm, indicating that P3HT can accelerate the generation of excitons in dye and increase the efficiency of charge separation upon illumination by light. Interestingly, the increment of IPCE in the absorption band 320–470 nm is higher than that in the band 470–720 nm. The former is associated with π–π* transitions of ancillary ligands as well as metal-to-ligand charge-transfer transitions toward ancillary ligands; the latter is associated with charge-transfer between the metal center and anchoring ligands [14]. This finding suggests that the use of P3HT as HTM enhances the rate of generation of photoexcited electrons in the ancillary ligands, which bear hexylthio-bithiophene moieties, more than it increases the rate of generation of the excited electrons in anchoring ligands, implying that P3HT more effectively reduces the cations on the ancillary ligands than it does those on the ruthenium.

Table 1
The photovoltaic characteristics of the four solid-state dye-sensitized solar cells based on TiO_2/CYC-B11/P3HT, TiO_2/CYC-B11/OMeTAD, TiO_2/Z907/P3HT and bare TiO_2/P3HT, and the values of charge-transfer resistance (R_{ct}) obtained by fitting the impedance spectra using an equivalent circuit.

Dye	HTMs	V_{OC} (V)	J_{SC} (mA cm^{-2})	*FF* (%)	η (%)	R_{ct} (Ω)
CYC-B11	P3HT	0.76	6.71	71.69	3.66	119
CYC-B11	OMeTAD	0.85	3.69	68.02	2.13	305
Z907	P3HT	0.75	3.13	62.50	1.47	242
–	P3HT	0.68	0.90	45.98	0.28	–

Electrochemical impedance spectroscopy is a powerful tool for characterizing charge-transfer and recombination kinetics in DSCs [20–22]. Herein, the impedance spectra of ss-DSCs were obtained using a potentiostate/galvanostat that was equipped with an FRA2 module by applying sinusoidal perturbations of ±10 mV at frequencies from 65 kHz to 10 mHz under constant light illumination of 100 mW cm^{-2}. The semicircle measured in the mid-range frequencies of 1–10^3 Hz is attributable to impedance that is associated with charge-transfer processes at the TiO_2/dye/HTM interface [23]. Fig. 7 displays the Nyquist plots of the three ss-DSCs; the symbols represent experimental data, while the solid lines plot the fit obtained by applying the equivalent circuit model in the inset. The charge-transfer resistance (R_{ct}) values of these devices were obtained from the diameter of the fitted semicircles, and are listed in Table 1. Among the three ss-DSCs, CYC-B11/P3HT has the smallest arc radius with an R_{ct} of 119 Ω, revealing smooth charge-transfer at the TiO_2/CYC-B11 and CYC-B11/P3HT interfaces that provides favorable efficiencies of dye regeneration and electron injection and thereby increases J_{SC}. This observation further suggests that

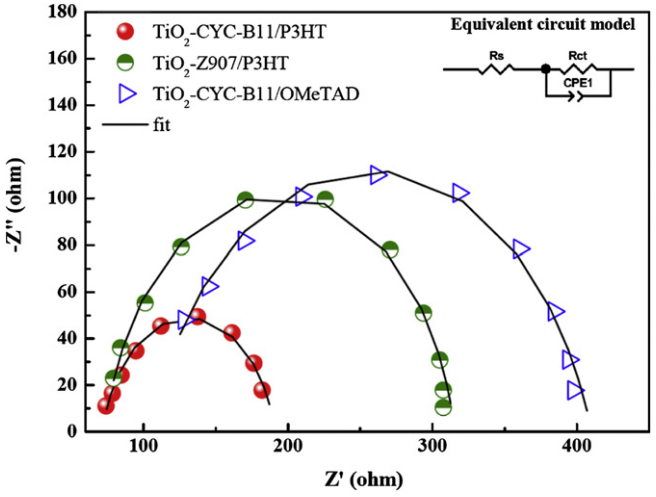

Fig. 7. Electrochemical impedance spectra of the three solid-state dye-sensitized solar cells based on TiO_2/CYC-B11/P3HT, TiO_2/CYC-B11/OMeTAD and TiO_2/Z907/P3HT. The inset presents the relevant equivalent circuit model.

a high structural similarity between the dye molecule and the hole transport material may enable the two materials to come into close contact at their interface, improving the reduction efficiency of dye cations.

4. Conclusions

The combination of a thiophene-bearing ruthenium complex, CYC-B11, as sensitizer with P3HT as HTM in the fabrication of ss-DSCs not only takes advantage of the combined light-harvesting capacity of two materials to generate more excitons but also reduces the charge-transfer resistance at the TiO_2/dye/HTM interfaces, considerably increasing J_{sc}. Consequently, the CYC-B11/P3HT device, based on an ultrathin ($\sim$0.5 μm) mesoporous TiO_2 layer, exhibits an outstanding PCE of 3.66% under AM 1.5 illumination. These results demonstrate that the structural compatibility between the dye molecules and HTM decisively influences the efficiency of dye regeneration. Accordingly, the use of dye molecules as sensitizer and colored conjugated molecules as HTM and co-sensitizer, in which both materials have complementary absorption spectra and high structural similarity, is essential to the development of high-efficiency ss-DSCs.

Acknowledgments

The authors thank National Taiwan University, National Central University, Academia Sinica, and the National Science Council of the Republic of China (NSC 100-3113-E-008-003) for financially supporting this research.

References

[1] L. Schmidt-Mende, S.M. Zakeeruddin, M. Grätzel, Appl. Phys. Lett. 86 (2005) 013504.
[2] H.J. Snaith, A.J. Moule, C. Klein, K. Meerholz, R.H. Friend, M. Grätzel, Nano Lett. 7 (2007) 3372–3376.
[3] N. Tétreault, E. Horváth, T. Moehl, J. Brillet, R. Smajda, S. Bungener, N. Cai, P. Wang, S.M. Zakeeruddin, L. Forró, A. Magrez, M. Grätzel, ACS Nano 4 (2010) 7644–7650.
[4] M. Wang, J. Liu, N.-L. Cevey-Ha, S.-J. Moon, P. Liska, R. Humphry-Baker, J.-E. Moser, C. Grätzel, P. Wang, S.M. Zakeeruddin, M. Grätzel, Nano Today 5 (2010) 169–174.
[5] N. Cai, S.-J. Moon, L. Cevey-Ha, T. Moehl, R. Humphry-Baker, P. Wang, S.M. Zakeeruddin, M. Grätzel, Nano Lett. 11 (2011) 1452–1456.
[6] M. Grätzel, MRS Bull. 30 (2005) 23–27.
[7] J. Melas-Kyriazi, I.-K. Ding, A. Marchioro, A. Punzi, B.E. Hardin, G.F. Bukhard, N. Tétreault, M. Grätzel, J.-E. Moser, M.D. McGehee, Adv. Energy Mater. 1 (2011) 407–414.
[8] A. Listori, B. O'Regan, Chem. Mater. 23 (2011) 3381–3399.
[9] S.A. Haque, T. Park, A.B. Holmes, J.R. Durrant, ChemPhysChem 1 (2003) 89–93.
[10] L. Schmidt-Mende, M. Grätzel, Thin Solid Films 500 (2006) 296–301.
[11] A. Abrusci, I.-K. Ding, M. Al-Hashimi, T. Segal-Peretz, M.D. McGehee, M. Heeney, G.L. Frey, H.J. Snaith, Energy Environ. Sci. 4 (2011) 3051–3058.
[12] H.J. Snaith, R. Humphry-Baker, P. Chen, I. Cesar, S.M. Zakeeruddin, M. Grätzel, Nanotechnology 8 (2008) 424003.
[13] I.-K. Ding, N. Tétreault, J. Brillet, B.E. Hardin, E.H. Smith, S.J. Rosenthal, F. Sauvage, M. Grätzel, M.D. McGehee, Adv. Funct. Mater. 19 (2009) 2431–2436.
[14] C.-Y. Chen, M. Wang, J.-Y. Li, N. Pootrakulchote, L. Alibabaei, C.-H. Ngoc-le, J.-D. Decoppet, J.-H. Tsai, C. Grätzel, C.-G. Wu, S.M. Zakkeeruddin, M. Grätzel, ACS Nano 3 (2009) 3103–3109.
[15] T.-A. Chen, R.D. Rieke, J. Am. Chem. Soc. 114 (1992) 10087–10088.
[16] K.-J. Jiang, K. Manseki, Y.-H. Yu, N. Masaki, K. Suzuki, Y.-L. Song, S. Yanagida, Adv. Funct. Mater. 19 (2009) 2481–2485.
[17] Q. Yu, S. Liu, M. Zhang, N. Cai, Y. Wang, P. Wang, J. Phys. Chem. C 113 (2009) 14559–14566.
[18] C. Goh, S.R. Scully, M.D. McGehee, J. Appl. Phys. 101 (2007) 114503.
[19] K.M. Coakley, Y. Liu, M.D. McGehee, K.L. Frindell, G.D. Stucky, Adv. Funct. Mater. 13 (2003) 301–306.
[20] H. Choi, S. Kim, S.O. Kang, J. Ko, M.-S. Kang, J.N. Clifford, A. Forneli, E. Palomares, M.K. Nazeeruddin, M. Grätzel, Angew. Chem. Int. Ed. 47 (2008) 8259–8263.
[21] Y.-H. Lai, C.-Y. Lin, J.-G. Chen, C.-C. Wang, K.-C. Huang, K.-Y. Liu, K.-F. Lin, J.-J. Lin, K.-C. Ho, Sol. Energy Mater. Sol. Cells 94 (2010) 668–674.
[22] R. Kern, R. Sastrawan, J. Ferber, R. Stangl, J. Luther, Electrochim. Acta 47 (2002) 4213–4225.
[23] L. Han, N. Koide, Y. Chiba, T. Mitate, Appl. Phys. Lett. 84 (2004) 2433–2435.